Peptide Binder to Glypican-3 as a Theranostic Agent for Hepatocellular Carcinoma

Fanching Lin*[1], Renee Clift*[1], Takeru Ehara[2], Hayato Yanagida[2], Steven Horton[1], Alain Noncovich[1], Matt Guest[1], Daniel Kim[1], Katrina Salvador[1], Samantha Richardson[1], Terra Miller[1], Guangzhou Han[1], Abhijit Bhat[1], Kenneth Song[1], and Gary Li[1]

[1]*RayzeBio, Inc., San Diego, California; and* [2]*PeptiDream Inc., Kanagawa, Japan*

Glypican-3 (GPC3) is a membrane-associated glycoprotein that is significantly upregulated in hepatocellular carcinomas (HCC) with minimal to no expression in normal tissues. The differential expression of GPC3 between tumor and normal tissues provides an opportunity for targeted radiopharmaceutical therapy to treat HCC, a leading cause of cancer-related deaths worldwide. **Methods**: DOTA-RYZ-GPC3 (RAYZ-8009) comprises a novel macrocyclic peptide binder to GPC3, a linker, and a chelator that can be complexed with different radioisotopes. The binding affinity was determined by surface plasma resonance and radioligand binding assays. Target-mediated cellular internalization was radiometrically measured at multiple time points. In vivo biodistribution, monotherapy, and combination treatments with ^{177}Lu or ^{225}Ac were performed on HCC xenografts. **Results:** RAYZ-8009 showed high binding affinity to GPC3 protein of human, mouse, canine, and cynomolgus monkey origins and no binding to other glypican family members. Potent cellular binding was confirmed in GPC3-positive HepG2 cells and was not affected by isotope switching. RAYZ-8009 achieved efficient internalization on binding to HepG2 cells. Biodistribution study of ^{177}Lu-RAYZ-8009 showed sustained tumor uptake and fast renal clearance, with minimal or no uptake in other normal tissues. Tumor-specific uptake was also demonstrated in orthotopic HCC tumors, with no uptake in surrounding liver tissue. Therapeutically, significant and durable tumor regression and survival benefit were achieved with ^{177}Lu- and ^{225}Ac-labeled RAYZ-8009, as single agents and in combination with lenvatinib, in GPC3-positive HCC xenografts. **Conclusion:** Preclinical in vitro and in vivo data demonstrate the potential of RAYZ-8009 as a theranostic agent for the treatment of patients with GPC3-positive HCC.

Key Words: GPC3; HCC; targeted radiotherapy; actinium; theranostics

J Nucl Med 2024; 65:586–592
DOI: 10.2967/jnumed.123.266766

Liver cancer is the sixth most diagnosed cancer and third most common cause of cancer deaths globally. In 2020, there were an estimated 905,677 new diagnoses and 830,180 deaths worldwide (*1*), and the incidence and mortality continue to worsen, likely because of an increase in nonalcoholic fatty liver disease (*2*). Of all liver cancer cases, hepatocellular carcinoma (HCC) accounts for approximately 85%. Although first-line systemic treatments such as atezolizumab/bevacizumab, tremelimumab-acti/durvalumab, and lenvatinib have shown encouraging clinical benefits in patients with unresectable HCC, more work is urgently needed to identify and exploit the vulnerabilities of HCC and improve treatment outcomes.

Glypican-3 (GPC3) is a membrane-associated heparan sulfate proteoglycan (*3*), involved primarily in embryonic development, and its expression levels decrease significantly after birth (*3*). Although barely detectable in normal adult tissues (*4*), a significant upregulation of GPC3 in HCC has been observed in up to 75% of cases (*5*–*7*) and appears to correlate with a poor prognosis (*8*,*9*). The expression of GPC3 can potentially be used to distinguish HCC from noncancerous pathologies such as focal nodular hyperplasia or cirrhosis (*10*,*11*). Besides HCC, GPC3 expression has also been observed in other adult and pediatric cancers, such as lung adenocarcinoma and squamous cell carcinoma (*12*,*13*), embryonal tumors (*14*), testicular germ cell tumors (*15*), and liposarcoma (*16*).

Because of its high expression in cancer and minimum expression in normal tissues, GPC3 is considered an attractive target for tumor-directed cancer therapy (*17*). Particularly, GPC3 CAR T-cell treatments have yielded promising results in both adult (*18*) and pediatric (*19*) HCC patients. Similarly, the differential expression also provides a basis for discovering and developing GPC3-targeted radiopharmaceutical therapy, especially for treatment-resistant or -refractory patients after first-line therapy to address disseminated disease and metastases (*20*). Previously, imaging studies with GPC3-targeted antibodies labeled with ^{124}I (*21*) or ^{89}Zr (*22*) have shown tumor-specific uptake with low background uptake. In this report, we describe in vitro, in vivo, and ex vivo characteristics of DOTA-RYZ-GPC3 (RAYZ-8009), a potent and selective GPC3 peptide binder, for treatment of HCC.

MATERIALS AND METHODS

Detailed reagents and experimental procedures are included in the supplemental materials and methods (supplemental materials are available at http://jnm.snmjournals.org).

Discovery of RAYZ-8009. RAYZ-8009 comprises a novel macrocyclic peptide binder to GPC3 and a chelator that binds radiometal isotopes. The GPC3 binder was discovered using the Peptide Discovery Platform System, a proprietary screening system of PeptiDream Inc. (*23*). From the initial library consisting of more than 1,013 unique peptides, GPC3-specific binders were enriched using His-tagged GPC3 (catalog no. 2119-GP; R&D Systems) immobilized on cobalt magnetic beads (Dynabeads [catalog no. 10103D]; Life Technologies Corp.) via iterative selection rounds (*24*,*25*). One of the enriched

Received Oct. 16, 2023; revision accepted Jan. 23, 2024.
For correspondence or reprints, contact Gary Li (gli@rayzebio.com).
*Contributed equally to this work.
Published online Feb. 29, 2024.

TABLE 1
Binding of RAYZ-8009 Conjugated with Different Stable Isotopes to HepG2 Cells

Compound	Inhibition constant (nM)	Half-maximal inhibitory concentration (nM)
^{175}Lu-RAYZ-8009	6.73	9.35
^{139}La-RAYZ-8009	11.19	15.67
^{69}Ga-RAYZ-8009	9.77	13.67

Binding affinity of ^{139}La-RAYZ-8009 and ^{69}Ga-RAYZ-8009 to human GPC3 was determined using competitive radioligand binding assay in HepG2 human HCC cells. ^{177}Lu-RAYZ-8009 was used as competitive radioligand, and ^{175}Lu-RAYZ-8009 was used as reference ligand.

peptides was further optimized chemically, and subsequent installation of a metal chelator afforded RAYZ-8009.

Cell Lines and Cell Culture. Human HCC cell lines were obtained from American Type Culture Collection, and the authentication and pathogen testing were performed at IDEXX Bio Research. Cells passaged fewer than 4 times were used for in vivo experiments.

Use of ^{139}La as Surrogate for ^{225}Ac. ^{139}La was used in place of ^{225}Ac in some nonclinical studies, as there is no stable isotope in the lanthanide series and La^{3+} is regarded as an appropriate surrogate for ^{225}Ac in preclinical studies (*26–28*).

Preparation of ^{177}Lu-RAYZ-8009 and ^{225}Ac-RAYZ-8009. RAYZ-8009 was labeled at a molar activity of 3.7 MBq/nmol (for in vitro and biodistribution studies) or 55.5 MBq/nmol (for efficacy studies) with [^{177}Lu]$LuCl_3$ (Isotopia). Quality control of ^{177}Lu-RAYZ-8009 was performed by radio–high-performance liquid chromatography with a reverse-phase C18 column at the end of synthesis. The ^{225}Ac ([^{225}Ac]$Ac(NO_3)_3$) was provided by the U.S. Department of Energy (managed by the National Isotope Development Center) and dissolved in 0.5 M HCl to form [^{225}Ac]$AcCl_3$. The [^{225}Ac]$AcCl_3$ solution was added to a reaction mixture consisting of sodium acetate (0.4 M) in water at pH 6.5. After the addition of RAYZ-8009, the reaction was incubated for 15 min at 90°C. Quality control of ^{225}Ac-RAYZ-8009 was performed by radio–thin-layer chromatography analysis, with silicic acid thin-layer chromatography plates as the solid phase and diethylenetriaminepentaacetic acid in water as the mobile phase, at the end of synthesis.

Biodistribution of ^{177}Lu-RAYZ-8009 in HepG2 Tumor–Bearing Mice. Animal studies were conducted under RayzeBio's animal care and use protocols. Biodistribution was studied on athymic nude mice harboring subcutaneously implanted HepG2 tumor. After single intravenous injections of 3.7 MBq (3.7 MBq/mmol) of ^{177}Lu-RAYZ-8009, tumor and normal tissues ($n = 3$) were collected at various time points and weighed, and the radioactivities were analyzed by γ-counting (Hidex). For dosimetry estimation, the time-integrated activity coefficient was obtained with monoexponential direct fitting and manual relative mass scaling and was used to estimate organ-specific absorbed doses in OLINDA.

SPECT Imaging. Static tumor images were acquired using the nanoSPECT imaging system (Mediso Imaging Systems). A whole-body CT scan was acquired (7 min, 50 kVp, and exposure time of 300 ms), followed by a static SPECT image (~20 min, multipinhole) with primary ^{177}Lu energy windows of 208 keV ± 10% (187–228 keV), 112 keV ± 10% (101–124 keV), and 56 keV (tertiary peak). For the subcutaneous HepG2 xenograft model, tumor-bearing mice received a bolus intravenous dose of 3.7 MBq of ^{177}Lu-RAYZ-8009 and were scanned 72 and 96 h after injection. For the orthotopic HepG2 model, tumor-bearing mice received a bolus intravenous dose of 3.7 MBq of ^{177}Lu-RAYZ-8009 and were scanned 2, 48, and 240 h after injection.

In Vivo Efficacy Studies. For the cell line–derived xenograft model, a cell suspension was diluted with RPMI medium containing 50% Matrigel (catalog no. 354234; Corning) to a concentration of 5×10^7 cells/mL. Athymic female nude mice were subcutaneously inoculated in the right hind flank with 5×10^6 cells per mouse. Tumor volume (mm^3) was assessed twice weekly and calculated as $width^2 \cdot length \cdot 0.5$. Animals were weighed individually on the days indicated in the graphs. Cage-side observations were performed daily on animals from the date of inoculation through study termination. Individual animals were killed when tumor volume reached about 2,000 mm^3, tumors became ulcerated, or the mice became moribund or had more than a 20% net weight loss lasting 3 d.

RESULTS

Binding Affinity and Specificity of RAYZ-8009 to GPC3

By surface plasma resonance, the binding equilibrium dissociation constant values of RAYZ-8009 were 0.35 and 0.42 nM for human and mouse GPC3, respectively (Supplemental Fig. 1).^{177}Lu-RAYZ-8009 bound to GPC3-expressing HepG2 cells with a dissociation constant of 10.8 nM as determined by a saturation radioligand binding assay (Supplemental Fig. 2). The binding between RAYZ-8009 and human GPC3 was not affected by the chelated isotopes ^{175}Lu, ^{139}La, or ^{69}Ga, as shown in Table 1 and Supplemental Figure 3, with comparable inhibition constants and half-maximal inhibitory concentrations measured by a competitive radioligand binding assay on HepG2 cells. Furthermore, RAYZ-8009 showed similar binding potencies to human, mouse, canine, and cynomolgus monkey GPC3 proteins (Table 2; Supplemental Fig. 4), which enables nonclinical pharmacokinetic and toxicity studies. In addition, ^{177}Lu-RAYZ-8009 exhibited binding specificity to GPC3, with no cross-reactivity to other human glypican family member proteins (Fig. 1).

Internalization of ^{177}Lu-RAYZ-8009

The internalized and surface-bound fractions of radioactivity were measured using a Microbeta counter (Perkin Elmer) at 20,

TABLE 2
Cross-Species Binding of ^{177}Lu-RAYZ-8009 to Recombinant Human, Mouse, Canine, and Cynomolgus Monkey GPC3

Parameter	Human GPC3	Mouse GPC3	Canine GPC3	Cynomolgus GPC3
Half-maximal effective concentration (nM)	1.92	1.33	5.73	4.42
Dissociation constant (nM)	2.08	1.37	5.40	3.97

Cross-species GPC3 binding of ^{177}Lu-RAYZ-8009 was evaluated in radioligand binding assay with recombinant mouse, canine, and cynomolgus monkey GPC3. Recombinant human GPC3 was used as positive control.

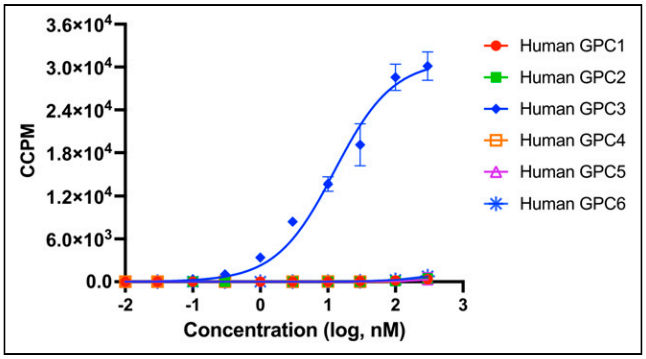

FIGURE 1. Binding specificity of ^{177}Lu-RAYZ-8009 among human glypican family proteins. Radioligand saturation binding of ^{177}Lu-RAYZ-8009 was determined with 5 μg/mL concentration of recombinant human GPC1, GPC2, GPC3, GPC4, GPC5, and GPC6 proteins. ^{177}Lu-RAYZ-8009 exhibited binding specificity to GPC3 with half-maximal effective concentration of 12.5 nM, without cross-reactivity to other human glypican proteins. CCPM = corrected counts per minute.

40, 60, 90, and 120 min after incubation of ^{177}Lu-RAYZ-8009 with HepG2 cells at 37°C. ^{177}Lu-RAYZ-8009 showed rapid internalization on binding to GPC3, with 41.6% internalized within 20 min and a peak internalization of 58.6% observed at 90 min (Fig. 2).

Pharmacokinetics in Mice

Plasma concentration–time curves for RAYZ-8009 are shown in Supplemental Figure 5. After intravenous administration at 5 mg/kg in female athymic nude mice, RAYZ-8009 showed a plasma clearance of 7.63 mL/min/kg and a half-life of 0.30 h. The volume of distribution was 0.172 L/kg, and the area under the plasma concentration–time curve from time zero to the last quantifiable concentration was 10,891 ng·h/mL. In both male and female C57BL/6 mice at 2 and 20 mg/kg doses of RAYZ-8009, the exposure appeared to be dose-proportional and independent of sex. The projected half-life in humans based on the mouse pharmacokinetic studies is about 2.2 h.

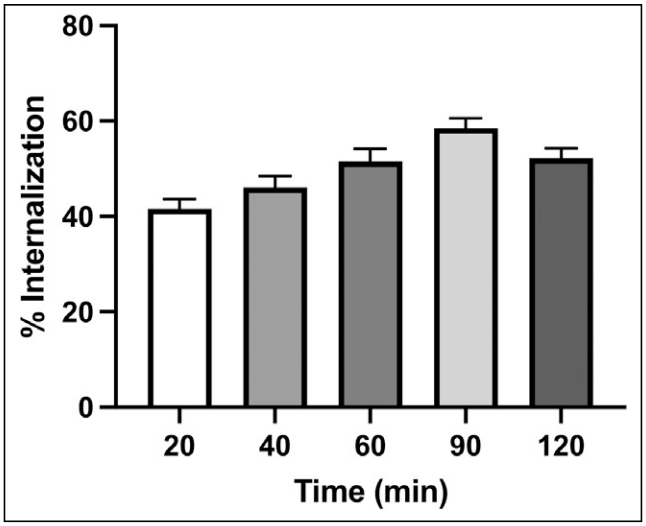

FIGURE 2. Internalization kinetics of ^{177}Lu-RAYZ-8009 in HepG2 cells. Internalized and surface-bound fractions of radioactivity were measured at indicated time points after incubation of ^{177}Lu-RAYZ-8009 with HepG2 cells at 37°C. Percentage internalization was calculated as ratio of internalized radioactivity to total (surface bound + internalized) activity. ^{177}Lu-RAYZ-8009 showed rapid internalization, with peak of 58.6% at 90 min.

Biodistribution and SPECT of ^{177}Lu-RAYZ-8009 in HepG2 Tumor–Bearing Mice

HepG2 tumor–bearing female athymic nude mice were intravenously dosed with a single injection of ^{177}Lu-RAYZ-8009 at a molar activity of 3.7 MBq/nmol. The mean injected activity was 3.9 MBq (3.7 MBq planned). Animals (3 per time point) were euthanized at 1, 2, 6, 24, 48, 96, 192, and 288 h after injection (Fig. 3A). The tumor-to-kidney ratios were 3.69, 11.33, 15.04, 22.29, and 12.37, with a tumoral percent injected dose per gram (%ID/g) of 16.63, 16.39, 8.76, 2.56, and 2.38, at 24, 48, 96, 192, and 288 h after dosing, respectively (Table 3). Kidney uptake was highest at 1 h after dosing and steadily declined throughout the 288-h study. By 96 h, the kidney levels dropped to 0.67 ± 0.16 %ID/g. The activity injected was cleared primarily in the first 24 h after dosing via excretion (71.40 %ID/g), with a smaller percentage recovered in kidneys (4.67 %ID/g) and other normal tissues (5.47 %ID/g) and the remainder retained in the tumor (16.63 %ID/g) (Table 3). Additionally, static tumor images were acquired at 72 and 96 h after dosing (Fig. 3B), confirming sustained tumor

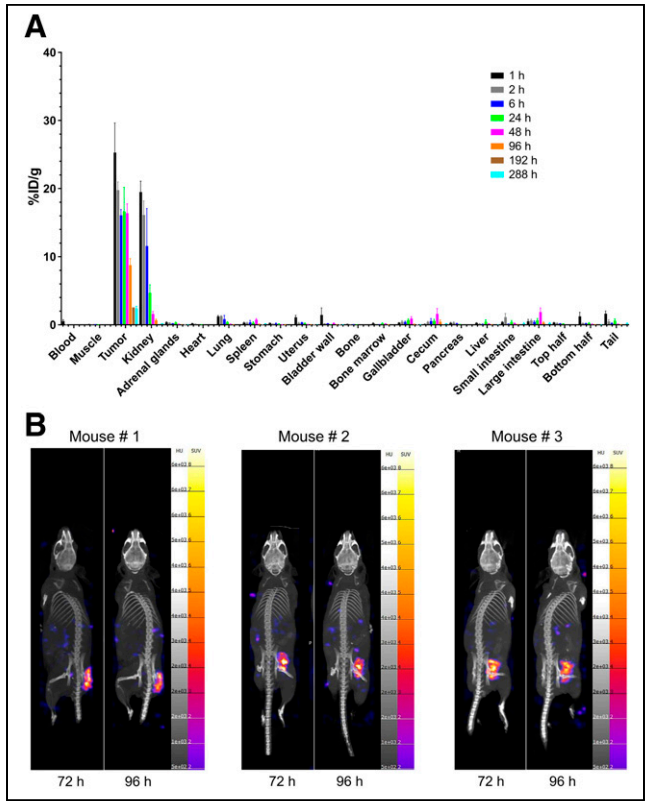

FIGURE 3. Biodistribution of ^{177}Lu-RAYZ-8009 in HepG2 xenograft model after single intravenous injection. (A) HepG2 tumor–bearing mice were intravenously dosed with ^{177}Lu-RAYZ-8009 (3.9 MBq, 3.7 MBq/nmol). Animals (3 per time point) were euthanized at indicated time points after injection. Various tissues were weighed, and radioactivities were measured by γ-counting. (B) Static tumor SPECT images were acquired at 72 and 96 h after dosing. %ID/g = percentage injected activity per gram; bottom half = remaining tissues not collected from directly below diaphragm to base of tail; top half = remaining tissues not collected from diaphragm to top of head.

TABLE 3
Ex Vivo Biodistribution After Single Intravenous Injection of ^{177}Lu-RAYZ-8009 to Female Nude Mice Bearing HepG2 Xenografted Tumor

	Average %ID/g							
Organ	1 h	2 h	6 h	24 h	48 h	96 h	192 h	288 h
Blood	0.54	0.03	0.01	0.01	0.01	0.00	0.00	0.00
Muscle	0.077	0.051	0.049	0.026	0.007	0.02	0.00	0.00
Tumor	25.28	19.77	16.08	16.63	16.39	8.76	2.56	2.38
Kidney	19.50	16.14	11.56	4.67	1.60	0.67	0.11	0.19
Adrenal glands	0.374	0.284	0.201	0.315	0.102	0.071	0.014	0.014
Heart	0.197	0.103	0.080	0.047	0.022	0.008	0.001	0.001
Lung	1.234	1.266	0.839	0.377	0.107	0.050	0.007	0.009
Spleen	0.314	0.273	0.348	0.285	0.740	0.075	0.028	0.116
Stomach	0.257	0.117	0.173	0.102	0.028	0.018	0.002	0.003
Uterus	1.097	0.269	0.325	0.189	0.071	0.058	0.026	0.043
Bladder wall	1.451	0.151	0.207	0.054	0.241	0.057	0.018	0.018
Bone	0.086	0.048	0.055	0.036	0.021	0.008	0.004	0.002
Bone marrow	0.228	0.104	0.067	0.176	0.139	0.025	0.003	0.000
Gallbladder	0.298	0.463	0.411	0.709	0.928	0.080	0.023	0.009
Cecum	0.106	0.402	0.573	0.575	1.621	0.456	0.095	0.159
Pancreas	0.279	0.308	0.175	0.076	0.023	0.009	0.001	0.000
Liver	0.263	0.133	0.090	0.463	0.159	0.060	0.020	0.044
Small intestine	0.403	1.126	0.138	0.415	0.208	0.077	0.022	0.184
Large intestine	0.532	0.621	0.451	0.634	1.872	0.306	0.107	0.248
Top half	0.326	0.227	0.186	0.143	0.047	0.016	0.003	0.006
Bottom half	1.235	0.250	0.183	0.246	0.097	0.055	0.012	0.017
Tail	1.645	0.506	0.234	0.593	0.120	0.057	0.015	0.166
Tumor-to-kidney ratio	1.29	1.25	1.76	3.69	11.33	15.04	22.29	12.37
Tumor-to-liver ratio	108.74	244.41	189.66	62.96	104.80	148.36	145.51	55.89

Top half = remaining tissues not collected from diaphragm to top of head; bottom half = remaining tissues not collected from directly below diaphragm to base of tail.

retention with minimal normal-tissue background uptake. Preliminary human dosimetry estimation based on HepG2 ex vivo biodistribution data indicated kidneys to be the dose-limiting organ (0.0858 Gy/GBq, vs. tumor at 0.779 G/GBq). When 23 Gy were used as the dose limit for kidneys, the maximal tumor dose was estimated to be about 209 Gy.

Tumor-Specific Uptake of ^{177}Lu-RAYZ-8009 in Orthotopic HepG2 HCC Model

Mice bearing orthotopically implanted HepG2 tumors were intravenously dosed with ^{177}Lu-RAYZ-8009 at 3.7 MBq/animal. Images were acquired at 2 h, 48 h, and 10 d after dosing (Supplemental Fig. 6). ^{177}Lu-RAYZ-8009 was confirmed to bind specifically to the tumor while sparing the surrounding normal liver tissue.

Antitumor Activity of ^{177}Lu- and ^{225}Ac-RAYZ-8009 in HepG2 Xenografts

HepG2 tumor–bearing mice (10/group) were administered a single intravenous dose of either ^{177}Lu-RAYZ-8009 (55.5 MBq/nmol) at 37 MBq/mouse or ^{225}Ac-RAYZ-8009 (0.185 MBq/nmol) at 0.0111, 0.0185, or 0.037 MBq/mouse. On day 26 (time of termination of vehicle group), ^{177}Lu-RAYZ-8009 exhibited 87.5% tumor growth inhibition (TGI) relative to vehicle, and ^{225}Ac-RAYZ-8009 achieved a 76.4%, 79.5%, or 85.1% TGI at 0.0111, 0.0185, or 0.037 MBq, respectively (Fig. 4A). At a dose 1,000 times lower, ^{225}Ac-RAYZ-8009 (0.037 MBq) was as efficacious in TGI as ^{177}Lu-RAYZ-8009 (37 MBq). No significant body weight change or clinical signs of stress were observed in any groups.

Antitumor Activity of ^{177}Lu- and ^{225}Ac-RAYZ-8009 in Hep3B Xenografts

Hep3B tumor–bearing mice (10/group) were dosed with ^{225}Ac-RAYZ-8009 (0.185 MBq/nmol) at 0.037 or 0.111 MBq/mouse or with ^{177}Lu-RAYZ-8009 (55.5 MBq/nmol) at 111 MBq/mouse. Treatment with RAYZ-8009 labeled with either isotope resulted in prolonged tumor regression (Fig. 4B). On day 22 after dosing (at the time of termination of the vehicle group), ^{177}Lu-RAYZ-8009 at 111 MBq resulted in a TGI of 109.8% relative to vehicle control, whereas ^{225}Ac-RAYZ-8009 at 0.111 or 0.037 MBq/mouse resulted in a TGI of 102.3% and 89.2%, respectively. At a dose 1,000 times lower, ^{225}Ac-RAYZ-8009 (0.111 MBq) was as efficacious in TGI as ^{177}Lu-RAYZ-8009 (111 MBq). Further tumor

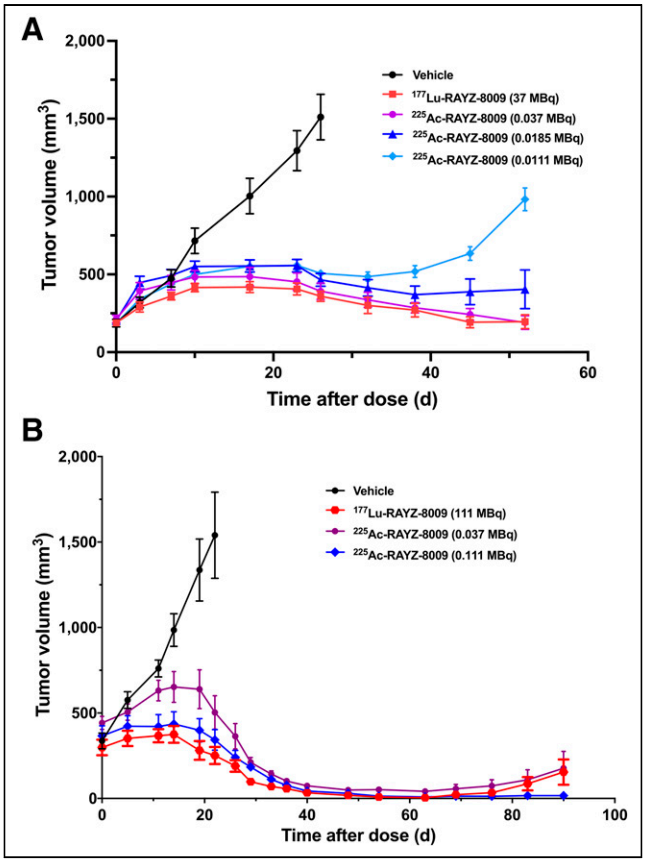

FIGURE 4. Antitumor activity of radiolabeled RAYZ-8009. (A) Antitumor activity of ^{177}Lu-RAYZ-8009 and ^{225}Ac-RAYZ-8009 in HepG2 xenografts that received single intravenous dose of either ^{177}Lu-RAYZ-8009 at 37 MBq/mouse or ^{225}Ac-RAYZ-8009 at 0.0111, 0.0185, or 0.037 MBq/mouse. (B) Antitumor activity of ^{177}Lu-RAYZ-8009 and ^{225}Ac-RAYZ-8009 in Hep3B xenografts that received single dose of ^{225}Ac-RAYZ-8009 at 0.037 or 0.111 MBq/mouse or ^{177}Lu-RAYZ-8009 at 111 MBq/mouse.

regression was observed in all treatment groups after day 22 for an additional 68 d. The most durable response was achieved with 0.111 MBq of ^{225}Ac-RAYZ-8009. No significant body weight change or clinical signs of stress were observed in any groups.

Antitumor Activity of ^{177}Lu- and ^{225}Ac-RAYZ-8009 When Combined with Lenvatinib

Lenvatinib is a standard-of-care therapy for advanced HCC. To study the potential of combining lenvatinib with RAYZ-8009, HepG2 tumor–bearing mice (10/group) were dosed with either vehicle, ^{177}Lu-RAYZ-8009 alone (11.1 MBq/mouse intravenously), lenvatinib alone (30 mg/kg orally every day for 10 d), or a combination of ^{177}Lu-RAYZ-8009 with lenvatinib. Treatment with lenvatinib alone and ^{177}Lu-RAYZ-8009 alone resulted in a 32% and 49% TGI, respectively, on day 36 after dosing (time of termination for the vehicle group), whereas the lenvatinib–^{177}Lu-RAYZ-8009 combination led to an improved TGI of 86% ($P < 0.0007$; Fig. 5A). In a separate study with Hep3B xenograft mice (10/group), treatment with lenvatinib alone (30 mg/kg orally every day for 10 d) and ^{225}Ac-RAYZ-8009 alone (0.0111 MBq/mouse) resulted in a 75% and 94% TGI, respectively, on day 24 after dosing (time of termination for the vehicle group), whereas the lenvatinib–^{225}Ac-RAYZ-8009 combination resulted in a TGI of 97% compared with vehicle alone

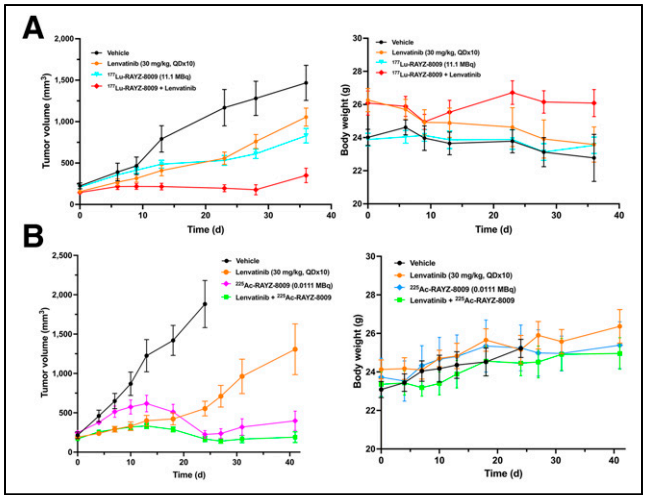

FIGURE 5. Antitumor activity of radiolabeled RAYZ-8009 in combination with lenvatinib. (A) Combination of ^{177}Lu-RAYZ-8009 and lenvatinib in HepG2 xenografts. Tumor-bearing mice were dosed with single intravenous injection of vehicle, ^{177}Lu-RAYZ-8009 alone (11.1 MBq/mouse), lenvatinib alone (30 mg/kg orally every day for 10 d), or combination of ^{177}Lu-RAYZ-8009 with lenvatinib. (B) Combination of ^{225}Ac-RAYZ-8009 and lenvatinib in Hep3B xenografts. Tumor-bearing mice were dosed with single intravenous injection of vehicle, ^{225}Ac-RAYZ-8009 alone (0.0111 MBq/mouse), lenvatinib alone (30 mg/kg orally every day for 10 d), or combination of ^{225}Ac-RAYZ-8009 with lenvatinib.

($P < 0.0009$; Fig. 5B). No significant body weight change or clinical signs of stress were observed in any groups.

DISCUSSION

Although many HCC cases can be attributed to liver cirrhosis and chronic liver diseases (*29*,*30*), GPC3 is detected only in HCC and not in cirrhotic liver tissue or other benign conditions (Supplemental Fig. 7) (*31*,*32*). Therefore, GPC3 can potentially serve as a diagnostic marker for distinguishing HCC from other non-HCC conditions (*10*,*11*). Besides HCC, other adult (*33*) and pediatric (*34*) cancer types that express GPC3 and can potentially benefit from a GPC3-directed theranostic approach include squamous lung cancer (*12*), embryonal tumors (*14*), testicular germ cell tumors (*15*), and liposarcoma (*16*).

Radiopharmaceutical therapy is a rapidly growing area in cancer drug development, with 2 agents (^{177}Lu-DOTATATE [Lutathera; Novartis] and ^{177}Lu-vipivotide tetraxetan [Pluvicto; Novartis]) having recently been approved by the Food and Drug Administration (*35*,*36*) and an ^{225}Ac-based radiopharmaceutical therapy being in phase 3 clinical evaluation (*37*,*38*). Peptide-based radiopharmaceuticals are preferred over antibodies because of several advantages, including better tumor penetration, ease of synthesis and modification, and low immunogenicity (*39*). However, previously reported GPC3 peptide binders appear to lack specificity or potency suitable for radiopharmaceutical therapy applications (*40*–*42*). In this study, RAYZ-8009 showed significantly higher affinity to GPC3 than other reported binders (*41*,*43*–*45*), an exquisite specificity to GPC3 with no binding to any other glypican family proteins, and compatibility with multiple radiometal isotopes. These properties make RAYZ-8009 suitable for theranostic development.

In tumor-bearing animals, ^{177}Lu-RAYZ-8009 exhibited sustained tumor-specific uptake and fast renal clearance. The sustained tumor

retention is likely the result of high binding affinity to GPC3 and efficient internalization. In line with minimal GPC3 expression in normal tissues by immunohistochemistry, there are minimal or undetectable signals in other normal tissues and organs except for the kidney, the primary route of clearance. Peptide uptake in the kidneys can also be due to kidney-expressed amino acid transporters and organic anion/cation transporters transiently binding the peptide (*46*,*47*). Even so, the HepG2 tumor signals were consistently higher than those in kidneys at all time points, with increasing tumor-to-kidney ratios ranging from 1.25 at 2 h to 22.29 at 192 h after injection.

In both HCC xenograft models, ^{225}Ac-RAYZ-8009 as a single agent demonstrated dose-dependent antitumor activities including sustained tumor regression. Compared with ^{177}Lu-RAYZ-8009, ^{225}Ac-RAYZ-8009 treatment yielded comparable TGI with an injected activity 1,000 times lower. The α-emitter ^{225}Ac-labeled binder may offer several advantages over the β-emitter ^{177}Lu-labeled binder. α-emitters typically have a short path in human tissue (40–100 μm), equivalent to the thickness of 1–3 cell widths, allowing for selective killing of targeted cancer cells while sparing surrounding healthy tissue (*48*). Additionally, α-emitters can generate linear energy transfer several magnitudes higher than β-emitters, causing double-stranded DNA breaks and subsequent cancer cell death with high efficiency (*49*,*50*). Along with higher linear energy transfer, the cell-killing effect of α-particles is not dependent on tumor oxidization status, whereas β-emitters are dependent on oxygen for maximal effect (*51*). Besides single-agent activity, RAYZ-8009 showed superior antitumor efficacy when combined with lenvatinib, one of the approved first-line therapies for unresectable HCC.

CONCLUSION

RAYZ-8009 is a peptide-based, potent, and selective radiopharmaceutical agent targeting GPC3-expression tumors. The favorable preclinical pharmacokinetic and biodistribution profiles, and durable antitumor efficacy either as a single agent or in combination with standard-of-care TKI inhibitor, demonstrate the potential of RAYZ-8009 as a theranostic agent for the treatment of patients with GPC3-positive HCC.

KEY POINTS

QUESTION: Does targeting of GPC3 overexpression with a radiopharmaceutical agent represent a promising therapeutic strategy for HCC?

PERTINENT FINDINGS: Treatment with the highly potent and selective GPC3-targeted peptide binder RAYZ-8009 conjugated with either ^{177}Lu or ^{225}Ac led to tumor-specific uptake of the agent, resulting in sustained tumor regression in HCC xenograft models.

IMPLICATIONS FOR PATIENT CARE: Preclinical data support clinical development of RAYZ-8009 as a theranostic agent for patients with HCC.

DISCLOSURE

Fanching Lin, Renee Clift, Steven Horton, Alain Noncovich, Matt Guest, Daniel Kim, Katrina Salvador, Samantha Richardson, Terra Miller, Guangzhou Han, Abhijit Bhat, Kenneth Song, and Gary Li are employees and stock option holders of RayzeBio, Inc. Takeru Ehara and Hayato Yanagida are employees of PeptiDream Inc. No other potential conflict of interest relevant to this article was reported.

ACKNOWLEDGMENTS

We thank Anna Karmann, Jessica Rearden, and Susan Moran for scientific and clinical input.

REFERENCES

1. Sung H, Ferlay J, Siegel RL, et al. Global cancer statistics 2020: GLOBOCAN estimates of incidence and mortality worldwide for 36 cancers in 185 countries. *CA Cancer J Clin.* 2021;71:209–249.
2. Eslam M, George J. Genetic contributions to NAFLD: leveraging shared genetics to uncover systems biology. *Nat Rev Gastroenterol Hepatol.* 2020;17:40–52.
3. Filmus J, Capurro M, Rast J. Glypicans. *Genome Biol.* 2008;9:224.
4. Haruyama Y, Kataoka H. Glypican-3 is a prognostic factor and an immunotherapeutic target in hepatocellular carcinoma. *World J Gastroenterol.* 2016;22:275–283.
5. Bell MM, Gutsche NT, King AP, et al. Glypican-3-targeted alpha particle therapy for hepatocellular carcinoma. *Molecules.* 2020;26:4.
6. Hsu H, Cheng W, Lai P. Cloning and expression of a developmentally regulated transcript MXR7 in hepatocellular carcinoma: biological significance and temporospatial distribution. *Cancer Res.* 1997;57:5179–5184.
7. Shih TC, Wang L, Wang HC, Wan YY. Glypican-3: a molecular marker for the detection and treatment of hepatocellular carcinoma. *Liver Res.* 2020;4:168–172.
8. Kaseb AO, Hassan M, Lacin S, et al. Evaluating clinical and prognostic implications of Glypican-3 in hepatocellular carcinoma. Vol 7; 2016:69916-69926.
9. Shirakawa H, Suzuki H, Shimomura M, et al. Glypican-3 expression is correlated with poor prognosis in hepatocellular carcinoma. *Cancer Sci.* 2009;100:1403–1407.
10. Capurro M, Wanless IR, Sherman M, et al. Glypican-3: a novel serum and histochemical marker for hepatocellular carcinoma. *Gastroenterology.* 2003;125:89–97.
11. Zhu ZW, Friess H, Wang L, et al. Enhanced glypican-3 expression differentiates the majority of hepatocellular carcinomas from benign hepatic disorders. *Gut.* 2001;48:558–564.
12. Aviel-Ronen S, Lau SK, Pintilie M, et al. Glypican-3 is overexpressed in lung squamous cell carcinoma, but not in adenocarcinoma. *Mod Pathol.* 2008;21:817–825.
13. Ning J, Jiang S, Li X, et al. GPC3 affects the prognosis of lung adenocarcinoma and lung squamous cell carcinoma. *BMC Pulm Med.* 2021;21:199.
14. Saikali Z, Sinnett D. Expression of glypican 3 (GPC3) in embryonal tumors. *Int J Cancer.* 2000;89:418–422.
15. Zynger DL, Dimov ND, Luan C, Teh BT, Yang XJ. Glypican 3: a novel marker in testicular germ cell tumors. *Am J Surg Pathol.* 2006;30:1570–1575.
16. Baumhoer D, Tornillo L, Stadlmann S, Roncalli M, Diamantis EK, Terracciano LM. Glypican 3 expression in human nonneoplastic, preneoplastic, and neoplastic tissues: a tissue microarray analysis of 4,387 tissue samples. *Am J Clin Pathol.* 2008;129:899–906.
17. Shimizu Y, Suzuki T, Yoshikawa T, Endo I, Nakatsura T. Next-generation cancer immunotherapy targeting glypican-3. *Front Oncol.* 2019;9:248.
18. Zhang Q, Fu Q, Cao W, et al. First report of preliminary safety, efficacy, and pharmacokinetics of C-CAR031 (GPC3-specific TGFβRIIDN CAR-T) in patients with advanced HCC [abstract]. *Cancer Res.* 2023;83(suppl):CT097.
19. Steffin DHM, Ghatwai N, Batra S, et al. A phase 1 clinical trial using armored GPC3-car T cells for children with relapsed/refractory liver tumors [abstract]. *J Clin Oncol.* 2020;37(suppl):TPS2647.
20. Pouget JP, Lozza C, Deshayes E, Boudousq V, Navarro-Teulon I. Introduction to radiobiology of targeted radionuclide therapy. *Front Med (Lausanne).* 2015;2:12.
21. Carrasquillo JA, O'Donoghue JA, Beylergil V, et al. I-124 codrituzumab imaging and biodistribution in patients with hepatocellular carcinoma. *EJNMMI Res.* 2018;8:20.
22. Fayn S, King AP, Gutsche NT, et al. Site-specifically conjugated single-domain antibody successfully identifies glypican-3-expressing liver cancer by immuno-PET. *J Nucl Med.* 2023;64:1017–1023.
23. Kashiwagi K, Reid CP, inventors; Peptidream Inc., assignee. Rapid display method in translational synthesis of peptide. Patent WO2011049157. April 28, 2011.
24. Goto Y, Katoh T, Suga H. Flexizymes for genetic code reprogramming. *Nat Protoc.* 2011;6:779–790.
25. Ishizawa T, Kawakami T, Reid PC, Murakami H. TRAP display: a high-speed selection method for the generation of functional polypeptides. *J Am Chem Soc.* 2013;135:5433–5440.
26. Nelson B, Andersson J, Wuest F. Targeted alpha therapy: progress in radionuclide production, radiochemistry and applications. *Pharmaceutics.* 2020;13:49.

27. Pandya DN, Hantgan R, Budzevich MM, et al. Preliminary therapy evaluation of ^{225}Ac-DOTA-c(RGDyK) demonstrates that Cerenkov radiation derived from ^{225}Ac daughter decay can be detected by optical imaging for in vivo tumor visualization. *Theranostics.* 2016;6:698–709.
28. Thiele NA, Wilson JJ. Actinium-225 for targeted alpha therapy: coordination chemistry and current chelation approaches. *Cancer Biother Radiopharm.* 2018;33:336–348.
29. McGlynn KA, Petrick JL, El-Serag HB. Epidemiology of hepatocellular carcinoma. *Hepatology.* 2021;73(suppl 1):4–13.
30. Chidambaranathan-Reghupaty S, Fisher PB, Sarkar D. Hepatocellular carcinoma (HCC): epidemiology, etiology and molecular classification. *Adv Cancer Res.* 2021;149:1–61.
31. Libbrecht L, Severi T, Cassiman D, et al. Glypican-3 expression distinguishes small hepatocellular carcinomas from cirrhosis, dysplastic nodules, and focal nodular hyperplasia-like nodules. *Am J Surg Pathol.* 2006;30:1405–1411.
32. Wang HL, Anatelli F, Zhai QJ, Adley B, Chuang ST, Yang XJ. Glypican-3 as a useful diagnostic marker that distinguishes hepatocellular carcinoma from benign hepatocellular mass lesions. *Arch Pathol Lab Med.* 2008;132:1723–1728.
33. Moek KL, Fehrmann RSN, van der Vegt B, de Vries EGE, de Groot DJA. Glypican 3 overexpression across a broad spectrum of tumor types discovered with functional genomic mRNA profiling of a large cancer database. *Am J Pathol.* 2018;188:1973–1981.
34. Ortiz MV, Roberts SS, Glade Bender J, Shukla N, Wexler LH. Immunotherapeutic targeting of GPC3 in pediatric solid embryonal tumors. *Front Oncol.* 2019;9:108.
35. Hennrich U, Kopka K. Lutathera®: the first FDA- and EMA-approved radiopharmaceutical for peptide receptor radionuclide therapy. *Pharmaceuticals (Basel).* 2019;12:114.
36. Hennrich U, Eder M. [^{177}Lu]Lu-PSMA-617 (Pluvicto™): the first FDA-approved radiotherapeutical for treatment of prostate cancer. *Pharmaceuticals (Basel).* 2022;15:1292.
37. Han G, Hwang E, Lin F, et al. RYZ101 (Ac-225 DOTATATE) opportunity beyond gastroenteropancreatic neuroendocrine tumors: preclinical efficacy in small cell lung cancer. *Mol Cancer Ther.* 2023;22:1434–1443.
38. Morris M, Ulaner GA, Halperin DM, et al. ACTION-1 phase Ib/3 trial of RYZ101 in somatostatin receptor subtype 2–expressing (SSTR2+) gastroenteropancreatic neuroendocrine tumors (GEP-NET) progressing after ^{177}Lu somatostatin analogue (SSA) therapy: initial safety analysis [abstract]. *J Clin Oncol.* 2023;41(suppl):4132.
39. Okarvi SM. Peptide-based radiopharmaceuticals and cytotoxic conjugates: potential tools against cancer. *Cancer Treat Rev.* 2008;34:13–26.
40. Berman RM, Kelada OJ, Gutsche NT, et al. In vitro performance of published glypican 3-targeting peptides TJ12P1 and L5 indicates lack of specificity and potency. *Cancer Biother Radiopharm.* 2019;34:498–503.
41. Wang S, Kalim M, Liang K, Zhan J. Polyclonal antibody production against rGPC3 and their application in diagnosis of hepatocellular carcinoma. *Prep Biochem Biotechnol.* 2018;48:435–445.
42. Li D, Li N, Zhang YF, et al. Persistent polyfunctional chimeric antigen receptor T cells that target glypican 3 eliminate orthotopic hepatocellular carcinomas in mice. *Gastroenterology.* 2020;158:2250–2265.e20.
43. Zhu D, Qin Y, Wang J, et al. Novel glypican-3-binding peptide for in vivo hepatocellular carcinoma fluorescent imaging. *Bioconjug Chem.* 2016;27:831–839.
44. Qin Z, Wang J, Wang Y, et al. Identification of a glypican-3-binding peptide for in vivo non-invasive human hepatocellular carcinoma detection. *Macromol Biosci.* 2017;17(4).
45. Zhang Q, Han Z, Tao J, et al. An innovative peptide with high affinity to GPC3 for hepatocellular carcinoma diagnosis. *Biomater Sci.* 2018;7:159–167.
46. Ganapathy V, Leibach FH. Carrier-mediated reabsorption of small peptides in renal proximal tubule. *Am J Physiol.* 1986;251:F945–F953.
47. van Montfoort JE, Hagenbuch B, Groothuis GM, Koepsell H, Meier PJ, Meijer DK. Drug uptake systems in liver and kidney. *Curr Drug Metab.* 2003;4:185–211.
48. Shi M, Jakobsson V, Greifenstein L, et al. Alpha-peptide receptor radionuclide therapy using actinium-225 labeled somatostatin receptor agonists and antagonists. *Front Med (Lausanne).* 2022;9:1034315.
49. Sgouros G. Dosimetry, radiobiology and synthetic lethality: radiopharmaceutical therapy (RPT) with alpha-particle-emitters. *Semin Nucl Med.* 2020;50:124–132.
50. Makvandi M, Dupis E, Engle JW, et al. Alpha-emitters and targeted alpha therapy in oncology: from basic science to clinical investigations. *Target Oncol.* 2018;13:189–203.
51. Wang H, Jiang H, Van De Gucht M, De Ridder M. Hypoxic radioresistance: can ROS be the key to overcome it? *Cancers (Basel).* 2019;11:112.